Frequency Selective Reflectarray Using Crossed-Dipole Elements With Square Loops for Wireless Communication Applications

Long Li, *Member, IEEE*, Qiang Chen, *Member, IEEE*, Qiaowei Yuan, Kunio Sawaya, *Senior Member, IEEE*, Tamami Maruyama, *Member, IEEE*, Tatsuo Furuno, *Member, IEEE*, and Shinji Uebayashi, *Member, IEEE*

***Abstract*—A new frequency selective reflectarray (FSR) comprising a crossed-dipole array and a frequency selective surface (FSS) of square loops printed on both sides of a dielectric substrate is presented for wireless communication applications. The reflectarray functions as a reflector, and generates the desired reflected beam shape while steering the primary wave source in the desired direction. Moreover, the FSR should be partially transparent for propagation channels of other communication systems working in other frequency bands. Some new FSR designs comprising 11 by 7 elements for dual-source and dual-polarized operation are given and verified by simulation and experiment. Furthermore, the FSR is applied to a WCDMA system to eliminate blind spots in communications between the base station and mobile users. A practical link budget analysis demonstrates the effectiveness of the FSR to improve the quality of communications. Finally, the proximity effect of concrete wall on the FSR is discussed to illustrate the applicability and flexibility of the proposed frequency selective reflectarray.**

***Index Terms*—Blindness, crossed-dipole, frequency selective reflectarray (FSR), link budget analysis, square-loop FSS, WCDMA.**

I. Introduction

A microstrip reflectarray is a flat low-profile reflector consisting of an array of microstrip patch elements that reflects a beam in a specified direction when illuminated by a primary source. The planar reflectarray is rapidly becoming an attractive alternative to the conventional parabolic reflector antenna because of its advantages such as the ability to surface mount the reflectarray due to its low mass and volume, its ease of deployment, low manufacturing cost, scannable beam, etc.

Manuscript received July 28, 2009; revised April 30, 2010; accepted June 23, 2010. Date of publication November 01, 2010; date of current version January 04, 2011. This work was supported in part by the Program for New Century Excellent Talents in University, China and in part by the National Natural Science Foundation of China under Contract 61072017.

L. Li is with School of Electronic Engineering, Xidian University, Xi'an 710071, China (e-mail: lilong@mail.xidian.edu.cn).

Q. Chen and K. Sawaya are with the Department of Electrical and Communication Engineering, Tohoku University, Sendai 980-8579, Japan (e-mail: chenq@ecei.tohoku.ac.jp; sawaya@ecei.tohoku.ac.jp).

Q. W. Yuan is with Sendai National College of Technology, Sendai 989-3128, Japan (e-mail: qwyuan@cc.sendai-ct.ac.jp).

T. Maruyama, T. Furuno, and S. Uebayashi are with NTT DoCoMo, Kanagawa 239-8536, Japan (e-mail: maruyamatam@nttdocomo.co.jp; furuno@nttdocomo.co.jp; uebayashi@nttdocomo.co.jp).

Color versions of one or more of the figures in this paper are available online at http://ieeexplore.ieee.org.

Digital Object Identifier 10.1109/TAP.2010.2090455

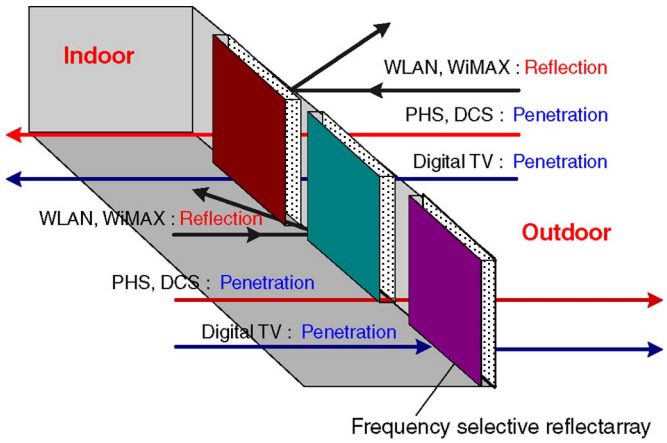

Fig. 1. Frequency selective reflectarray surface mounted onto walls for reflection and penetration of different communication systems.

[1]–[3]. In wireless communications such as in a large-scale indoor/outdoor base station in a wireless local area network (WLAN) or distributed control system (DCS), planar reflectarray antennas can be mounted on the ceiling or a house wall to reflect beams covering different areas, especially blind spots for the primary source. It is also desirable that the reflectarray minimizes blockage of propagation channels from other communication systems, as illustrated in Fig. 1.

The conventional microstrip reflectarray consists of an array of microstrip patches or dipoles printed on a thin metal-grounded dielectric substrate the role of which is to convert a spherical wave produced by a feed antenna into a plane wave. The concept of the reflectarray is based on phase compensation for each element dimension to achieve cophase reradiation and to concentrate the scattered wave toward a specific direction. Many phasing schemes have been recently developed [1]–[11]. The most common approach is to use identical patches with different-length transmission delay lines attached to the patches for phase compensation [1], [3]. Other approaches include the use of different sized patches without delay lines to introduce a nearly in-phase aperture [4]–[6] or using variable rotation angles of a patch [7].

In this paper, a new idea for a reflectarray design is presented in that the reflectarray can function as a reflector, and generate the desired reflection beam shape and direction for a primary wave source, while achieving partial transparency for propagation channels of other communication systems working in other frequency bands. A microstrip reflectarray using crossed-dipole

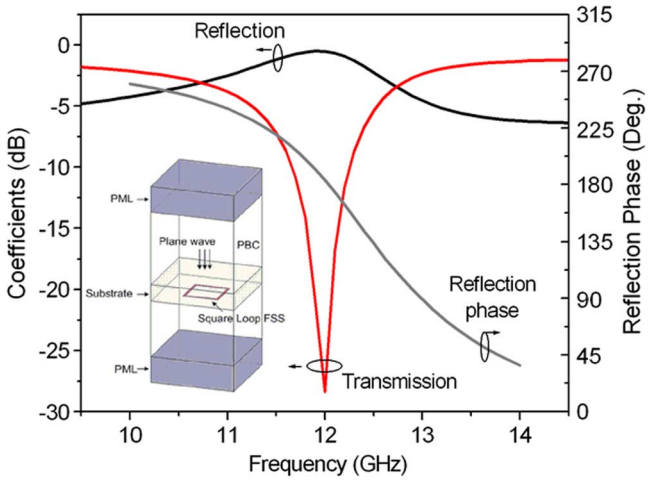

Fig. 2. Reflection and transmission coefficients of square-loop FSS using an infinite periodic model.

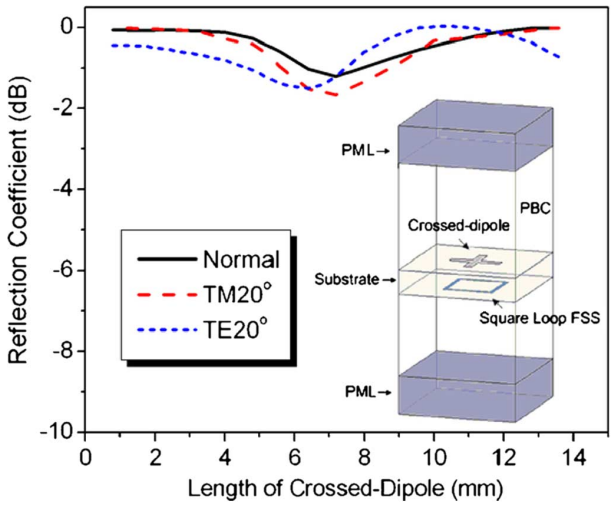

Fig. 3. Reflection coefficients versus length of crossed-dipole elements at 12 GHz using CGP-500 substrate.

elements with a frequency selective surface (FSS) comprising square loops is designed to demonstrate the effectiveness of the proposed idea. In Section II, an infinite periodic model is used to analyze the reflection and transmission coefficients of the new crossed-dipole elements with a square-loop FSS. Section III presents an analysis and design of the frequency selective reflectarray (FSR) using crossed-dipole elements with a square-loop FSS. The properties of the new reflectarray are discussed and compared to those of the conventional microstrip reflectarray. We experimentally verified the radiation pattern and transmission coefficient of the FSR with 11 by 7 elements. New designs for dual-source and dual-polarized FSR are given in Section IV. Furthermore, an FSR is designed and applied to a WCDMA system for eliminating blindness of communications between the base station and mobile users. A practical link budget analysis described in Section V shows the effectiveness of the FSR to improve the quality of communications. Finally, Section VI discusses the influence of the presence of a concrete wall on the FSR, when the FSR is surface mounted in the proximity of a house wall.

II. Crossed-Dipole Elements With Square-Loop FSS

An FSS is a surface that exhibits different reflection and/or transmission properties as a function of frequency [12]. An array of loops acts as a band-stop filter, which is characterized by the fundamental resonance of loops when the circumference of the elements is approximately one wavelength in the dielectric surrounding them. An infinite periodic model using the HFSS simulation [13] was performed to analyze the reflection and transmission coefficients of the square-loop FSS, as shown in Fig. 2, in which periodic boundary conditions (PBCs) are assumed around the unit cell. The period in both the x and y directions is $\mathrm{D} = 14\,\mathrm{mm}$ and the circumference of the square loop is 23.8 mm. The square-loop array is attached to the bottom surface of a dielectric substrate that is $t = 3.2\ \mathrm{mm}$ thick and has a relative permittivity of $\varepsilon_r = 2.6$ (CGP-500 with a loss tangent of 0.0018). The reflection and transmission coefficients of the square-loop FSS versus the frequency are shown in Fig. 2. It can be seen that a total reflection occurs at the resonant frequency of 12 GHz, and the reflection phase is 180°. Considering this feature, a metal ground plane of the microstrip reflectarray can be replaced with the loop-FSS for a certain frequency band.

In this work, a new reflectarray comprising a printed crossed-dipole array and square-loop FSS on opposite surfaces of the dielectric substrate is proposed and designed. First, the effect of the crossed-dipole array on the square-loop FSS should be considered. Fig. 3 shows the reflection coefficients of the composite unit cell versus the length of the crossed-dipole elements for different incidence angles and polarizations at 12 GHz. This figure shows that the variation in the reflection loss is within 2 dB for both TE and TM polarizations, when the length of the crossed-dipole elements varies from the minimum length of 0.5 mm to the maximum length of 13.6 mm. We analyzed the effect of mutual coupling between the crossed-dipole elements and the square-loop FSS based on the reflection coefficient, as shown in Fig. 4. It can be found that the mutual coupling is very strong when the substrate thickness is thin, especially when the length of the crossed-dipole elements is approximately half a dielectric wavelength. This results in significant leakage of energy. When the thickness is increased, the performance is favorable for designing a reflectarray of varying dipole lengths.

III. Analysis and Design of FSR Using Crossed-Dipole Elements With Square-Loop FSS

The key technique in the design of a reflectarray is how the individual elements are designed to scatter the incident wave with the proper phase compensation to produce a beam toward a specific direction. The configuration of the frequency selective reflectarray is shown in Fig. 5. The reradiated field from the crossed-dipole in an arbitrary direction, $\hat{u}$, will be of the form [1]

$$E(\hat{u}) = \sum_{m=1}^{M}\sum_{n=1}^{N} F(\vec{r}_{mn}\cdot\vec{r}_f)A(\vec{r}_{mn}\cdot\hat{u}_0)A(\hat{u}\cdot\hat{u}_0) \cdot \exp\left\{-jk_0\left[|\vec{r}_{mn}-\vec{r}_f| + \vec{r}_{mn}\cdot\hat{u}\right] + j\phi_{mn}\right\} \quad (1)$$

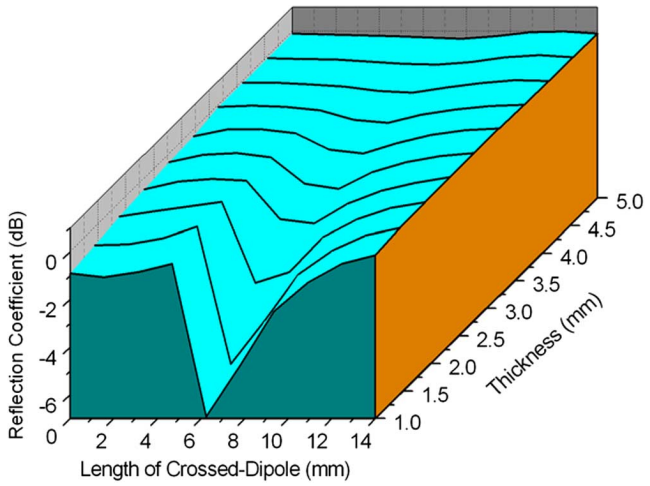

Fig. 4. Reflection coefficient characteristics versus the length of crossed-dipole elements and substrate thickness.

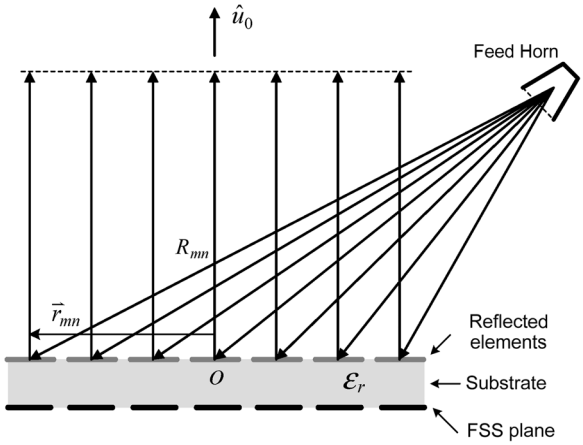

Fig. 5. Configuration of frequency selective reflectarray.

where F is the feed pattern function, A is the pattern function of the crossed-dipole elements. $\vec{r}_{mn}$ and $\vec{r}_f$ are the position vectors of the mn_{th} element and the feed horn antenna, respectively. $\hat{u}_0$ is the desired main-beam pointing direction of the reflectarray. ϕ_{mn} is the required phase of the scattered field from the mn_{th} element. The conditions that enable an array aperture distribution to be cophase in the desired direction $\hat{u}_0$ are given by [11]

$$\phi_{mn} - k_0(R_{mn} + \vec{r}_{mn} \cdot \hat{u}_0) = 2p\pi, \quad p = 0, \pm 1, \pm 2, \cdots \quad (2)$$

where R_{mn} is the distance from the feed source to the mn_{th} array element, i.e., $R_{mn} = |\vec{r}_{mn} - \vec{r}_f|$. The wave number is given as $k_0 = \omega_0/c$. It is noted that ω_0 is the working frequency of the FSS ground.

In the design of microstrip reflectarray, the dimensions or the shape of the reflecting elements must be changed in order to obtain the required reflection phase. The compensated phase curve can be calculated by analyzing the infinite periodic array of identical microstrip elements [13]. After obtaining the phase curve, the resonant length of the mn_{th} element is determined to produce a phase shift, ϕ_{mn}, in the field scattered from the element. Fig. 6 shows the reflection phase curve of the crossed-dipole element with square-loop FSS. Compared to the reflection phase curve of the crossed-dipole elements with a conventional ground plane, it can be found that the proposed element structure has a slowly varying phase curve, which yields a reduction in the phase error caused by fabrication error in element size in practice. Generally, the phase of the reflection coefficient is dependent not only on the element size but also on the angle of incidence of plane wave. However, it was shown that the reflection phases are not greatly affected by the incidence angles, even when the incidence angle is more than 45° [4], [14]. In this study, taking into account the grating lobe criteria $(D/\lambda < 1/(1+\sin\theta_0))$, the scan angle for the reflectarray designed here is restricted to less than or equal to 45°. Therefore, the FSR was simply designed based on the reflection phase characteristics of a plane wave that is normal incident.

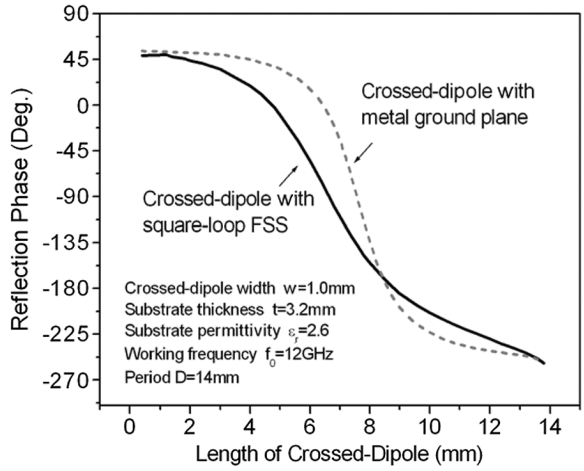

Fig. 6. Comparison of reflection phase of crossed-dipole with square-loop FSS and metal ground plane.

In order to validate the element structure of the crossed-dipole elements with the square-loop FSS, a 30°-beam-steering reflectarray along the x-axis operating at 12 GHz was designed. When we use higher frequency to keep enough bandwidth for achieving high-speed broadband mobile communication systems, it is a significant problem that radio waves can not reach out-of-sight areas. To address the problem, we proposed to use a passive reflector that enables to control the reflected wave direction and coverage. Here we adopt 12 GHz for this study. Fig. 7(a) and (b) show the top and bottom surfaces of the reflectarray geometry using 11×7 crossed dipoles of variable size and a square-loop FSS, respectively. The element spacing is 0.56λ in both the x and y directions. The substrate thickness and relative permittivity are assumed to be $t = 3.2$ mm and $\varepsilon_r = 2.6$, respectively. The feed may be positioned at an arbitrary angle and distance from the reflectarray, while it should be sufficiently far away from the reflectarray so that the incident wave can be treated as a plane wave. In the present design, the incident plane wave arrives from y-axis direction of $(\theta_i, \varphi_i) = (20°, -90°)$ in the corresponding spherical coordinate, and the main beam is scanned in x-axis direction of $(\theta_r, \varphi_r) = (30°, 0°)$. The incidence plane wave can be either TM or TE polarized due to the symmetric crossed-dipole design. The dimensions of all elements are determined based on (2) and Fig. 6.

A full-wave simulation using HFSS for the radiation pattern in the xoz plane with an incident TE-polarized plane wave was performed. The results are shown in Fig. 8. In order to verify the

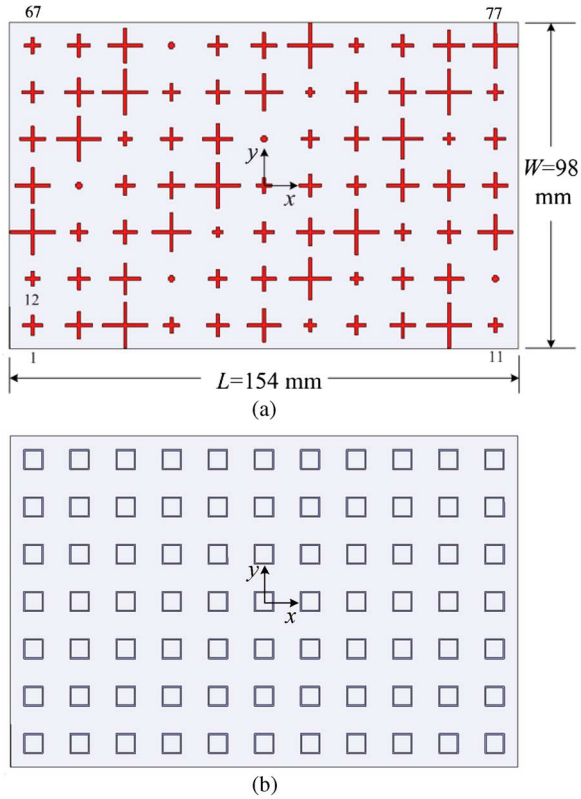

Fig. 7. (a) Crossed-dipole array on the top of designed reflectarray. (b) Square-loop FSS on the bottom of designed reflectarray.

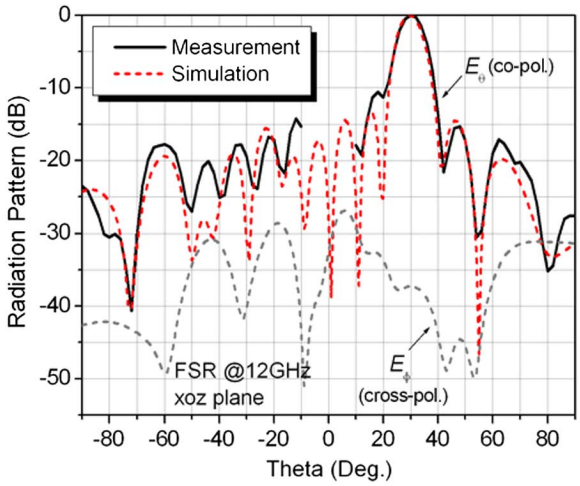

Fig. 8. Comparison of simulation and measurement results of radiation pattern in xoz plane of the designed FSR.

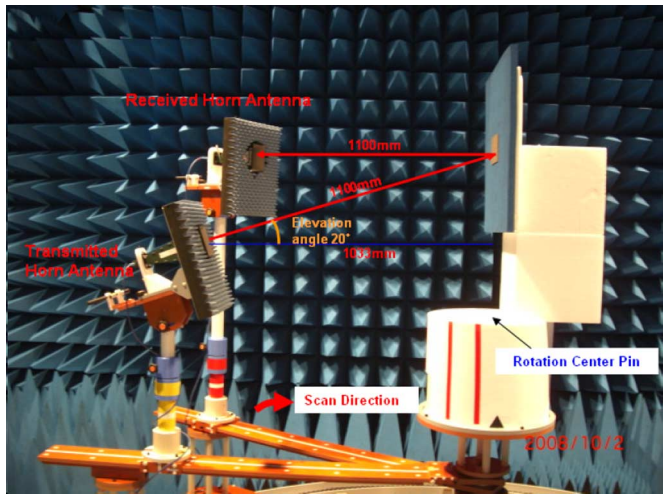

Fig. 9. Measurement system for reflectarray at NTT DoCoMo, Kanagawa.

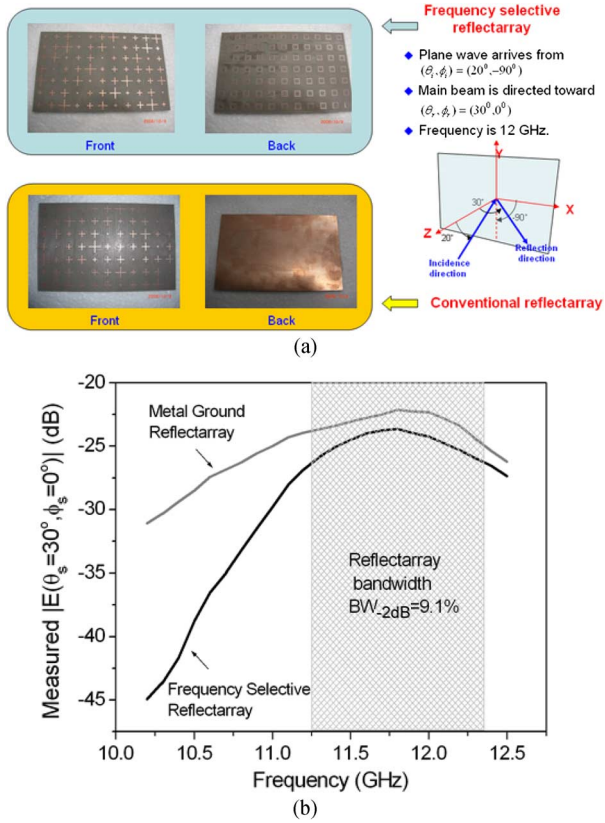

Fig. 10. (a) Experimental models of FSR and conventional metal ground reflectarray. (b) Comparison of measured electrical field magnitude of the two reflectarrays in the direction of the main beam.

design, we fabricated the FSR and conducted experiments. The measurement of the radiation pattern was performed in an anechoic chamber at NTT DoCoMo, Kanagawa, Japan. The configuration for the measurement is shown in Fig. 9. For comparison, the measurement results are also shown in Fig. 8. It should be noted that a small azimuth region of approximately 20 degrees can not be measured due to the mechanical limitation of turntable in this measurement system, nonetheless, the measurement results are in good agreement with the simulation results. Both the measurement and simulation results show that the main beam is directed at 30°. Thus, the reflectarray using the crossed-dipole array with the square-loop FSS satisfies the requirements regarding the main beam position very well. The performance and design for the TM-polarized incidence waves can be similarly obtained due to symmetry [9].

To compare the loop FSS reflectarray and the conventional metal ground plane reflectarray based on the directivity bandwidth, an 11×7 crossed-dipole reflectarray with a metal ground plane was also designed and simulated. as shown in Fig. 10(a). Fig. 10(b) shows the measured electrical field magnitude in the direction of the main beam for two kinds of reflectarrays for

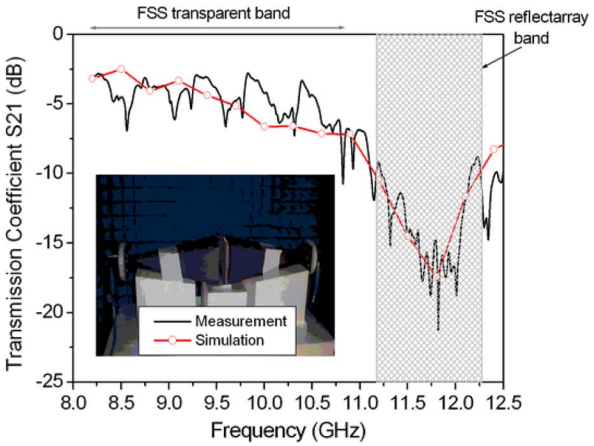

Fig. 11. Measured transmission coefficient S21 of the FSR versus frequency of in near-zone using a pair of standard-gain horn antennas.

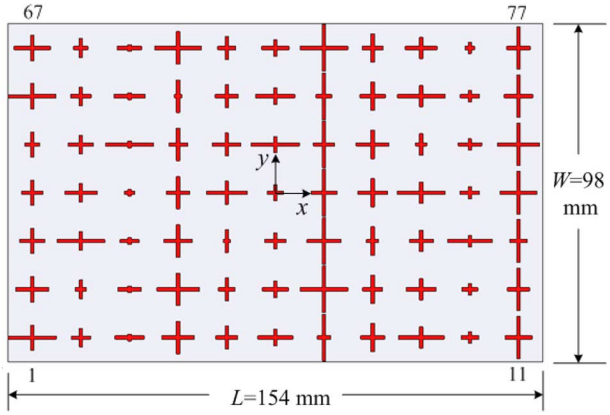

Fig. 12. Top surface of dual-source and dual-polarization operation FSR, and bottom surface is still a square-loop FSS, which is the same in Fig. 7(b).

an incident TE-polarized plane wave, which represents the performance of the directivity against frequency. Directivity of the reflectarray can be defined as the ratio of the scattered intensity in the direction of the main beam from the reflectarray to the scattered intensity averaged over all directions [15]. As shown in Fig. 10(b), below the working frequency of the loop FSS, the directivity of the designed reflectarray drops suddenly, which indicates that the incidence wave partly penetrates through the reflectarray. In other words, the reflectarray is partially transparent to lower frequency band waves compared to the operating frequency, resulting in a reduction in the blockage effect to other communication systems. The -2 dB directivity-drop bandwidth of the reflectarray is approximately 9.1%. However, the maximum directivity of the FSR is about 1.5 dB less than that for the metal ground reflectarray. This is due to the incomplete reflection of the frequency selective surface in an actual environment. Some leakage is inevitable.

Furthermore, a near-zone transmission measurement was performed to verify the frequency selective characteristics of the FSR. The results are shown in Fig. 11. The FSR and conventional reflectarray were placed between a pair of standard gain horn antennas (8.2 GHz–12.5 GHz) for transmission measurement, respectively. Since the dimensions of the experimental models are relatively small, the measurement distance was set in the near-zone. Although it is not very accurate, this experiment can provide insight into the frequency selective characteristics of the FSR. Fig. 11 shows that when the working frequency is outside the FSS band, the FSR is partially transparent to other wave sources.

IV. Dual-Source and Dual-Polarized FSR

By using non-symmetric crossed dipoles, we can design a new FSR with dual-source and dual-polarized operation, as shown in Fig. 12. The bottom surface is still a square-loop FSS, which is the same as that in Fig. 7(b). The material used to fabricate this FSR is also CGP-500. The design target is aimed to dual-source and dual polarized incidence. One incidence source is from $(\theta_{i1}, \varphi_{i1}) = (20°, -90°)$ with horizontal polarization, and the main beam is steered in the direction of $(\theta_{r1}, \varphi_{r1}) = (40°, 0°)$. Meanwhile, the other incidence source is from $(\theta_{i2}, \varphi_{i2}) = (30°, -180°)$ with vertical polarization, and the main beam is scanned in the direction of $(\theta_{r2}, \varphi_{r2}) = (0°, 0°)$, i.e., normal reflection. In the first case, only horizontal dipole elements along the x-axis will be excited, but in the second case, only vertical dipole elements along the y-axis will be excited. According to the orthogonality of the crossed-dipole elements, the two polarizations are independent, even if the two sources are excited simultaneously. Tables I and II give the dimensions of all dipoles along the x- and y-axes, respectively. Both simulations and experiments demonstrate the performance of the dual-source and dual-polarized FSR, as shown in Fig. 13. It is noted that an additional beam at around 30 deg is observed in the Fig. 13(b), which is due to the measuring system error. Because the transmitted and received horn antennas are located at the same incidence plane in this case, the conventional reflected wave based on the Snell reflection law from testing targets except the FSR is also detected.

V. Link Budget Analysis in WCDMA System

In wideband wireless communications for mobile users, eliminating the blind spots of a base station antenna in a densely populated downtown district is a significant problem. Generally, RF boosters are used to extend the cellular coverage area, but standard RF boosters require transceivers, power supplies, cables, etc., which incur a high cost and have large requirements in terms of installation space. Considering the wireless communication system model shown in Fig. 14 [14], a planar reflectarray is used as a reflector that is set on the top of a building or surface mounted onto a wall. Through proper design, it can steer the main beam to cover the blind spots of base station antennas. The merits of parallel installation are that we can take into account quake-resistance standards and integrate the equipment with surrounding environment such as into billboards [10]. However, if a metallic reflector is used, it is very difficult to direct the reflected beam in a specified direction even if using a tilt adjuster.

A frequency selective reflectarray was designed and applied to a wideband CDMA (WCDMA) system. The WCDMA (Rel.99) system requires a paired spectrum: one band (1920–1980 MHz) for uplinks and one (2110–2170 MHz) for downlinks [16]. Here the central operating frequency of

TABLE I
DIMENSIONS OF HORIZONTAL DIPOLES (UNIT: mm)

Row / Column	1	2	3	4	5	6	7
1	13.8	9.56	7.36	6.07	4.41	13.8	10.6
2	5.66	3.27	13.8	9.29	7.25	5.96	4.15
3	8.46	6.83	5.53	2.87	13.8	9.03	7.13
4	9.41	12.3	8.29	6.73	5.43	2.25	13.5
5	6.36	4.90	2.05	11.8	8.12	6.63	5.27
6	10.2	7.59	6.26	4.75	13.8	11.4	7.95
7	3.89	13.8	9.84	7.46	6.16	4.56	13.8
8	7.03	5.75	3.55	13.8	9.51	7.34	6.05
9	13.2	8.62	6.92	5.64	3.21	13.8	9.25
10	5.15	4.63	12.7	8.43	6.81	5.51	2.76
11	7.82	6.45	5.02	10.5	12.2	8.25	6.71

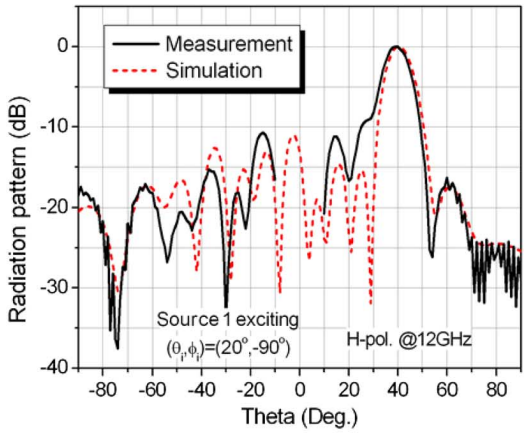

(a)

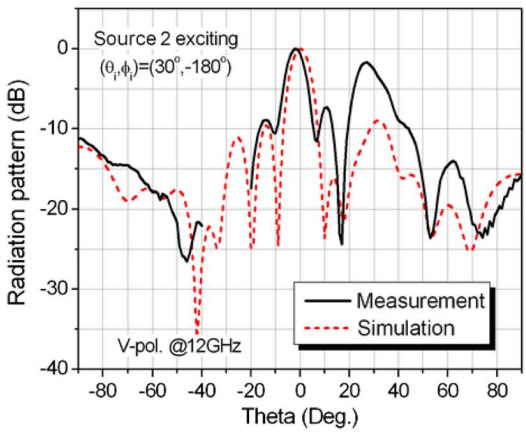

(b)

Fig. 13. Measured and simulated radiation patterns of dual-source and dual-polarized FSR, (a) Excited Source 1 with H-pol. (b) Excited Source 2 with V-pol.

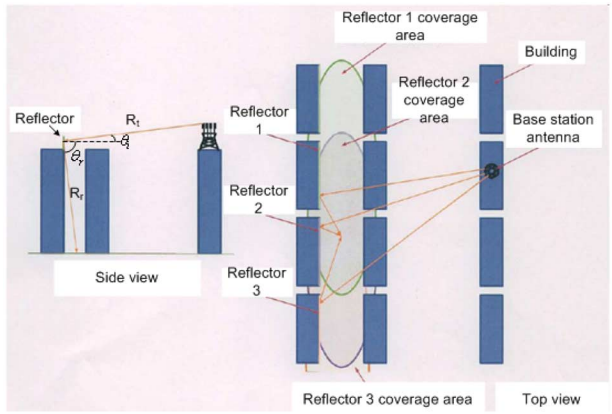

Fig. 14. Elimination of blindness using reflectarrays in wireless communication system.

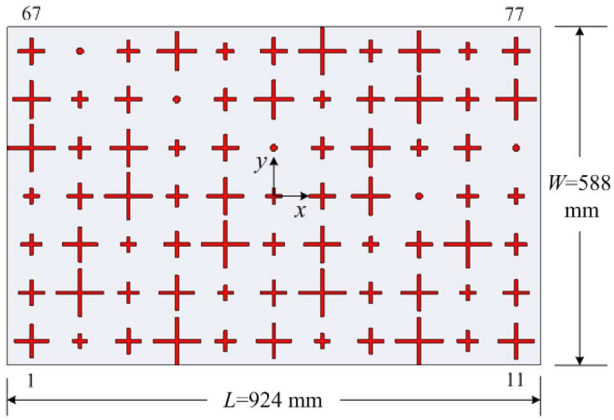

Fig. 15. Frequency selective reflectarray of 11 by 7 elements at working frequency of 2 GHz.

the FSR is set to 2000 MHz and the required bandwidth must be greater than 10% to cover both the uplink and downlink spectra. According to previous design methods and frequency transformation schemes, we designed a 45°-beam-steering FSR that functions at 2 GHz. For the downlink, a plane wave is transmitted from a base station antenna at the incidence angle of $(\theta_i, \varphi_i) = (20°, -90°)$ to the FSR and the reflected main-beam is steered 45° in the xoz plane, and vice versa for the uplink. The FSR with 11 by 7 elements is shown in Fig. 15.

For convenient verification through experiments, a scale-down model working at 12 GHz is fabricated and measured, which means that all dimensions of the crossed-dipole reflectarray and square-loop FSS are one sixth of those in Fig. 15. So the whole size of the reflectarray is $Ls = 154$ mm and $\mathrm{Ws} = 98$ mm. The substrate thickness is $t = 3.2$ mm, and permittivity is still 2.6 (CGP-500). Fig. 16(a) shows the measured and simulated radiation patterns of the reflectarray in the xoz plane. The figure shows that the designed FSR clearly

TABLE II
DIMENSIONS OF VERTICAL DIPOLES (UNIT: mm)

Row / Column	1	2	3	4	5	6	7
1	7.33	7.33	7.33	7.33	7.33	7.33	7.33
2	5.46	5.46	5.46	5.46	5.46	5.46	5.46
3	2.05	2.05	2.05	2.05	2.05	2.05	2.05
4	9.47	9.47	9.47	9.47	9.47	9.47	9.47
5	6.76	6.76	6.76	6.76	6.76	6.76	6.76
6	4.75	4.75	4.75	4.75	4.75	4.75	4.75
7	13.6	13.6	13.6	13.6	13.6	13.6	13.6
8	8.31	8.31	8.31	8.31	8.31	8.31	8.31
9	6.25	6.25	6.25	6.25	6.25	6.25	6.25
10	3.39	3.39	3.39	3.39	3.39	3.39	3.39
11	12.3	12.3	12.3	12.3	12.3	12.3	12.3

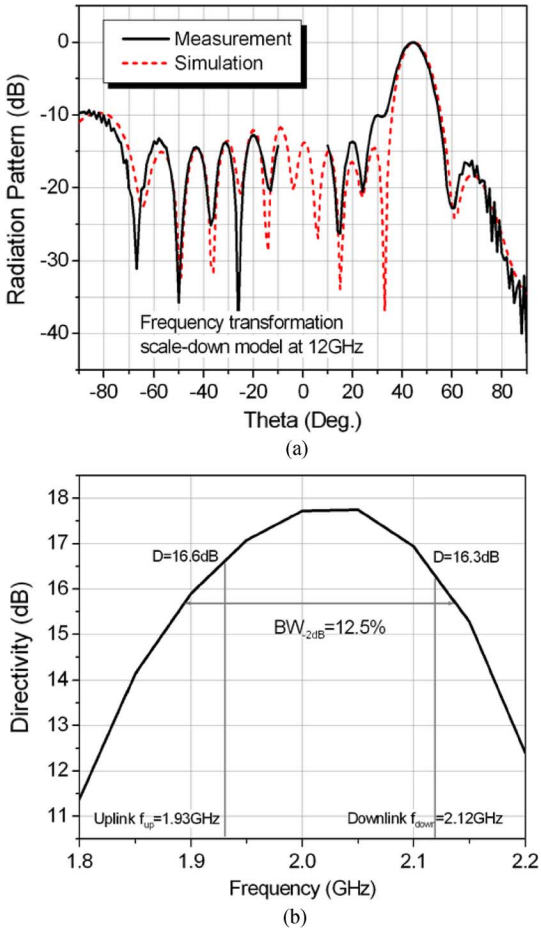

Fig. 16. (a) Measured and simulated radiation patterns of the scaled-down model of reflectarray at 12 GHz. (b) Directivity of designed WCDMA reflectarray versus frequency.

satisfies the requirement regarding the main beam position. Fig. 16(b) shows the computed directivity against the frequency. As shown in the figure, the -2 dB directivity-drop bandwidth of 12.5% is achieved to cover the uplink and downlink spectra.

To demonstrate the elimination of the blind spots using the reflectarray in the model of the wireless communication system

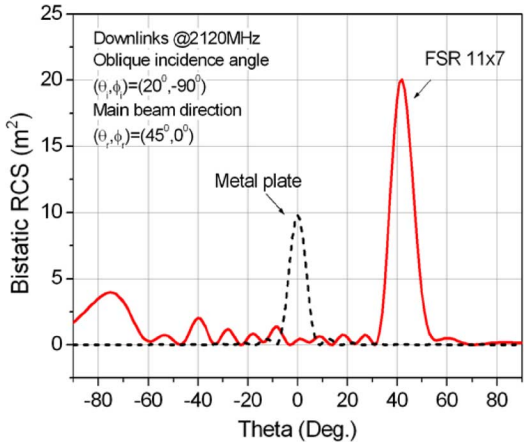

Fig. 17. Bistatic RCS of FSR and metal plate with the same dimensions for downlink at 2120 MHz.

shown in Fig. 14, we give a simple link budget analysis for the WCDMA (Rel.99) system. We consider in radar range equation

$$P_r = \left(\frac{P_t G_t}{4\pi R_t^2}\right) \cdot \left(\frac{\sigma}{4\pi R_r^2}\right) \cdot \left(\frac{G_r \lambda^2}{4\pi}\right) \tag{3}$$

where the first item represents the power density incident on the reflectarray, the second item indicates the scattering power density at the receiver from the reflectarray, and the third item denotes the effective area of the receiver antenna. Term σ is the bistatic radar cross section (RCS) of the reflectarray. The bistatic RCS of the FSR functioning at 2120 MHz in the downlink is shown in Fig. 17. For comparison, the bistatic RCS of a metal plate with the same dimensions as the reflectarray is also given in Fig. 17.

Considering conventional cellular mobile communications, we assume the maximum R_t and R_r are 500 meters and 40 meters, respectively. Generally, the transmitter and receiver antenna gains are 10 dBi and 0 dBi, respectively. Therefore, we can predict the maximum propagation loss $(PL = P_t/P_r)$ [16] by using various reflectors, as shown in Fig. 18. The dashed line shown in Fig. 18 represents the threshold of the propagation loss. Blind spots occur if the propagation loss is greater than the value of 128 dB. The results show that if we use an FSR with 11×7 elements, the signal propagation loss can be reduced

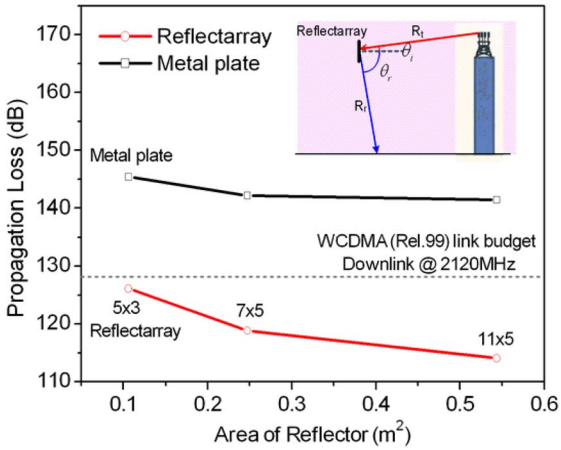

Fig. 18. Link budget analysis of propagation gain in WCDMA (Rel. 99) system using various reflectors.

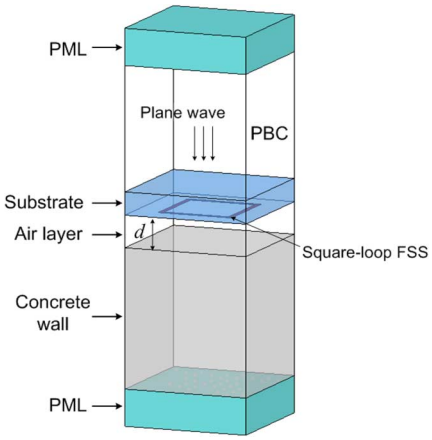

Fig. 19. Infinite periodic model of square-loop FSS with concrete wall for reflection and transmission analysis.

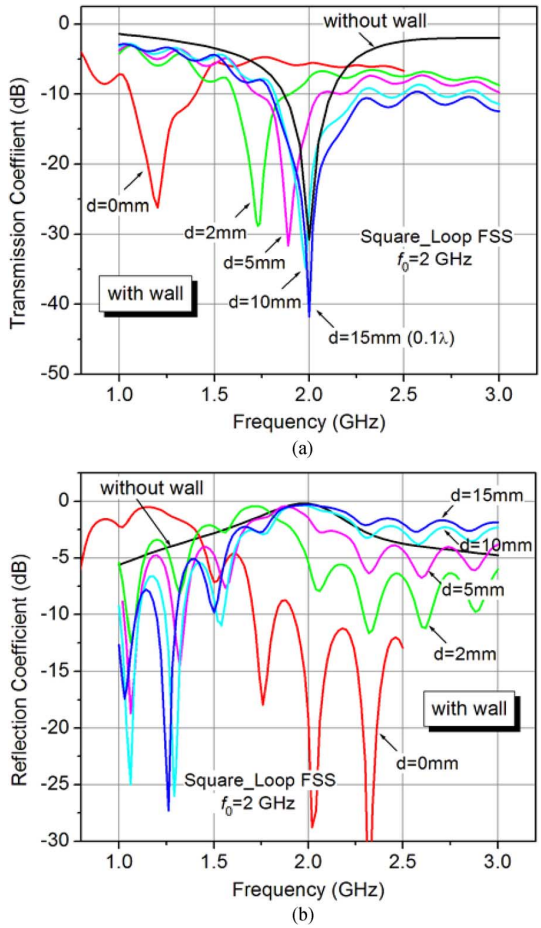

Fig. 20. Frequency response of square-loop FSS with concrete wall under various parameter values of d. (a) Transmission coefficient, (b) Reflection coefficient.

effectively, which successfully eliminates the blindness in the original communication environment. However, when using a metal plate as the reflector, it does not work even if the size of the plate is increased. Similar conclusions for the uplink can be obtained, which demonstrate the effectiveness of the proposed reflectarray.

VI. Discussion of Proximity Effect of Concrete Wall

One of advantages of microstrip reflectarray is surface mountable with lower mass and volume. The possible applications are shown in Figs. 1 and 14, where the FSR is surface mounted onto a house wall for indoor and outdoor wireless communications. Meanwhile, we should take into account the proximity effect of concrete wall on the FSR in a practical application, because the presence of the wall will change the frequency response of the square-loop FSS. Considering the infinite periodic model shown in Fig. 19, we analyze the transmission and reflection characteristics of the square-loop FSS in the proximity of a concrete wall. The central working frequency is set to 2 GHz for the WCDMA system.

Generally, the effective relative permittivity of a concrete wall is $\varepsilon_r = 7 - j0.3$ at around 2 GHz [17], and the wall thickness varies from 20 mm to 300 mm. In this paper, we choose the wall thickness is 200 mm. For the sake of convenient reference, we assume a parameter of d to represent the distance between the square-loop FSS and the concrete wall. If $d = 0$, it means that the FSS contacts the wall, and if $d > 0$, there is an air layer between the FSS and the wall, which is usually consistent with the facts. The period in both the x and y directions is $\mathrm{D} = 84$ mm and the circumference of the square loop is 146.4 mm. The square-loop array is attached to the bottom surface of a dielectric substrate that is $t = 19.2$ mm thick and has a relative permittivity of $\varepsilon_r = 2.6$ (CGP-500 with a loss tangent of 0.0018). Fig. 20(a) and (b) show the simulated frequency response of transmission and reflection coefficients under various parameter values of d. As a reference, the transmission and reflection characteristics of the same square-loop FSS but without wall are also shown in Fig. 20.

It can be seen that the presence of a concrete wall really affects the frequency response of the square-loop FSS, especially in close proximity to the wall. When $d = 0$, the resonant frequency of the square-loop FSS is moved to 1.2 GHz. However, by adjusting the thickness of air layer, when $d = 15$ mm (i.e., $0.1\lambda_0$), the resonant frequency will return to 2 GHz. In this case, the reflection coefficient is still very good, only -0.284 dB at 2 GHz. It should be pointed out that the reflection coefficient of the original square-loop FSS without wall is -0.185 dB

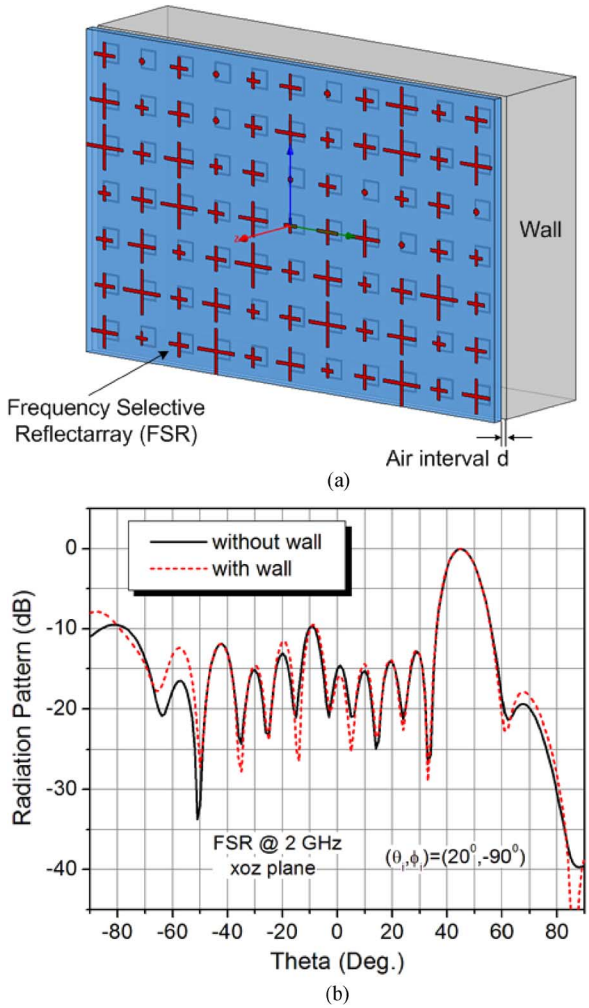

Fig. 21. (a) Simulation model of the FSR surface mounted on concrete wall; (b) Comparison of radiation patterns of the FSR with and without wall.

at 2 GHz. Furthermore, it is shown that the wave penetration through the FSS and wall is still excellent to low-frequency band, but some attenuation to high-frequency band due to the loss of a concrete wall.

The FSR with 11 by 7 elements shown in Fig. 15 was designed for WCDMA system without considering the influence of a wall. When the FSR is applied to a practical environment, it can be surface mounted on a wall but with an air interval of 15 mm. A plane wave is transmitted from a base station antenna at the incidence angle of $(\theta_i, \varphi_i) = (20°, -90°)$ to the FSR and the reflected main-beam is steered 45° in the xoz plane. The simulation model is shown in Fig. 21(a), and the radiation pattern of the FSR with wall is shown in Fig. 21(b). For a comparison, the simulated radiation pattern of the FSR without wall is also shown in this figure. It can be seen that the influence of the wall on the FSR turns out to be negligible in such case. The designed FSR with/without wall clearly satisfies the requirement regarding the main beam position.

Based on the analysis above, we have known that when d is greater than or equal to 0.1 central operating wavelength, the influence of a wall on the FSR is less. Therefore, the design principal and method of a FSR can be independent on the wall

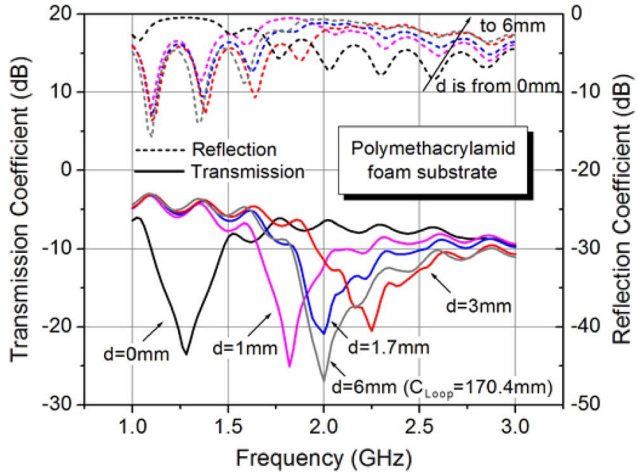

Fig. 22. Reflection and transmission coefficients of the square-loop FSS in close proximity to a wall, in which the substrate is made of a low permittivity foam material, i.e., polymethacrylamid hard foam.

in such conditions. It is applicable to the practical engineering when the FSR is surface mounted on a wall with an air interval of 15 mm.

Furthermore, it can be seen from Fig. 20 that the FSS will resonant at lower frequency when it is placed in close proximity to a concrete wall. Therefore, we may utilize more practical and low-cost substrates to design a FSR, such as polymethacrylamid hard foam ($\varepsilon_r = 1.07$, $\tan\delta = 8 \times 10^{-4}$) [18]. The various thicknesses of this foam are available. Fig. 22 shows the reflection and transmission properties of the square-loop FSS which is attached to the bottom surface of a polymethacrylamid hard foam with thickness of 19.2 mm. It is found that the resonant frequency of the FSS could return to 2 GHz by adjusting the air-layer thickness to the correct fit, as $d = 1.7$ mm. It is worth pointing out that we make use of the interaction between the FSS and the wall (i.e. proximity effects) to design a FSR in this case. But for the previous design shown in Fig. 21, we would like to eliminate or degrade the proximity effects of a wall by inserting a thick layer of air.

It is helpful for decreasing the insertion loss to properly increase the thickness of air-layer, while the dimension of the square-loop should be adjusted to resonate at operating frequency in that case, as illustrated in Fig. 22. Therefore, it is more flexible to design a FSR in practical applications when we take the proximity effect of the wall and parameter d into account.

VII. Conclusion

This paper presented a new concept for designing a frequency selective reflectarray (FSR) for wireless communication applications. The FSR has the ability to function as a reflector and steer reflected beam for a special frequency-band wave, while achieving partial transparency for the other frequency-band waves. A simple example of a reflectarray, which consists of a printed crossed-dipole array with a square-loop FSS on the opposite surface of the dielectric substrate, was presented to indicate the feasibility. The designed symmetric crossed-dipole FSR is independent of polarization. Measurement results

agree well with the simulation results, which show that the performance of the FSR satisfies the requirements for the main beam position very well. A new design for the FSR using non-symmetric crossed dipoles, which can be used for dual-source and dual-polarized operation with two main beams simultaneously, was proposed and tested. Furthermore, the FSR was implemented in a WCDMA system to eliminate the blind spots in wireless mobile communications. A link budget analysis of propagation loss has demonstrated the effectiveness of the proposed frequency selective reflectarray. When the FSR is surface mounted onto a house wall in practical applications, the proximity effect of the concrete wall on the FSR should be considered. The analyzed results indicate that it is more flexible to design the FSR by introducing an air interval between the wall and FSR.

ACKNOWLEDGMENT

The authors gratefully acknowledge the helpful comments and suggestions provided by reviewers.

REFERENCES

[1] J. Huang, Analysis of a microstrip reflectarray antenna for microspacecraft applications TDA Progress Rep. 42-120, Feb. 1995, pp. 153–173.
[2] D. M. Pozar, T. S. Targonsky, and H. D. Syrigos, "Design of millimeter wave microstrip reflectarrays," *IEEE Trans. Antennas Propag.*, vol. 45, no. 2, pp. 287–295, 1997.
[3] D. C. Chang and M. C. Huang, "Multiple-polarization microstrip reflectarray antenna with high efficiency and low cross-polarization," *IEEE Trans. Antennas Propag.*, vol. 43, pp. 829–834, Aug. 1995.
[4] S. D. Targonski and D. M. Pozar, "Analysis and design of a microstrip reflectarray using patches of variable size," in *IEEE AP-S/URSI Int. Symp. Dig.*, Seattle, WA, Jun. 20–24, 1994, pp. 1820–1823.
[5] J. A. Encinar, "Design of two-layer printed reflectarrays using patches of variable size," *IEEE Trans. Antennas Propag.*, vol. 49, pp. 1403–1410, Oct. 2001.
[6] D. Pilz and W. Menzel, "Full wave analysis of a planar reflector antenna," in *Proc. Asia-Pacific Microwave Conf.*, Dec. 2–5, 1997, pp. 225–227.
[7] J. Huang and R. J. Pogorzelski, "A ka-band microstrip reflectarray with elements having variable rotation angles," *IEEE Trans. Antennas Propag.*, vol. 46, pp. 650–656, May 1998.
[8] D. M. Pozar and S. D. Targonski, "A microstrip reflectarray using crossed dipoles," in *Proc. IEEE Antennas and Propagation Society Int. Symp.*, Jun. 21–26, 1998, vol. 2, pp. 1008–1011.
[9] L. Li, Q. Chen, Q. W. Yuan, K. Sawaya, T. Maruyama, T. Furuno, and S. Uebayashi, "Microstrip reflectarray using crossed-dipole with frequency selective surface of loops," presented at the Int. Symp. on Antenna and Propagation (ISAP2008), Taipei, Taiwan, Oct. 27–30, 2008.
[10] T. Maruyama, T. Furuno, and S. Uebayashi, "Experiment and analysis of reflect beam direction control using a reflector having periodic tapered mushroom-like structure," presented at the Int. Symp. on Antenna and Propagation (ISAP2008), Taipei, Taiwan, Oct. 27–30, 2008.
[11] K. W. Lam, "On the Analysis and Design of Microstrip Reflectarrays," Ph.D. dissertation, City University of Hong Kong, Kowloon, 2002.
[12] B. A. Munk, "Frequency-selective surfaces and periodic structures," in *Antennas for All Applications*, J. D. Kraus, Ed., R. J. Marhefka, Ed., 3rd ed. New York: McGraw-Hill, 2002.
[13] R. Remski, "Analysis of PBG surfaces using Ansoft HFSS," *Microwave J.*, vol. 43, no. 9, pp. 190–198, Sep. 2000.
[14] L. Li, Q. Chen, Q. W. Yuan, K. Sawaya, T. Maruyama, T. Furuno, and S. Uebayashi, "Novel broadband planar reflectarray with parasitic dipoles for wireless communication applications," *IEEE Antennas Wireless Propag. Lett.*, vol. 8, pp. 881–885, 2009.
[15] C. A. Balanis, *Antenna Theory Analysis and Design*, 3rd ed. Hoboken, NJ: Wiley, 2005.
[16] H. Holma and A. Toskala, *WCDMA for UMTS: HSPA Evolution and LTE*, 4th ed. Hoboken, NJ: Wiley, 2007.
[17] E. Richalot, M. Bonilla, M. F. Wang, V. Fouad-Hanna, H. Baudrand, and J. Wiart, "Electromagnetic propagation into reinforced-concrete walls," *IEEE Trans. Microwave Theory Tech.*, vol. 48, no. 3, pp. 357–366, Mar. 2000.
[18] J.-F. Zurcher, "The SSFIP: A global concept for high performance broadband planar antennas," *Electron. Lett.*, vol. 24, no. 23, pp. 1433–1435, Nov. 1988.

Long Li (M'06) was born in Guizhou, China. He received the B.E. and Ph.D. degrees in electromagnetic fields and microwave technology from Xidian University, Xi'an, China, in 1998 and 2005, respectively.

He joined the School of Electronic Engineering, Xidian University, in 2005 and was promoted to Associate Professor in 2006. He was a Senior Research Associate in the Wireless Communications Research Center, City University of Hong Kong, in 2006. He received the Japan Society for Promotion of Science (JSPS) Postdoctoral Fellowship and visited Tohoku University, Sendai, Japan, as a JSPS Fellow from Nov. 2006 to Nov. 2008. He is currently a Professor in the School of Electronic Engineering, Xidian University. His research interests include computational electromagnetics, electromagnetic compatibility, and novel artificial metamaterials.

Dr. Li received the Nomination Award of National Excellent Doctoral Dissertation of China in 2007 and won the Best Paper Award in the International Symposium on Antennas and Propagation in 2008. He received the Program for New Century Excellent Talents in University of the Ministry of Education of China in 2010. He is a senior member of the Chinese Institute of Electronics (CIE) and the Institute of Electronics, Information and Communication Engineers (IEICE) of Japan.

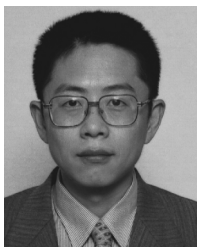

Qiang Chen (M'94) received the B.E. degree from Xidian University, Xi'an, China, in 1986, and the M.E. and D.E. degrees from Tohoku University, Sendai, Japan, in 1991 and 1994, respectively.

He is currently an Associate Professor with the Department of Electrical Communications, Tohoku University. His primary research interests include computational electromagnetics, array antennas, and antenna measurement.

Dr. Chen received the Young Scientists Award in 1993, the Best Paper Award and Zen-ichi Kiyasu Award in 2009 from the Institute of Electronics, Information and Communication Engineers (IEICE) of Japan. He is a member of the IEICE. He served as the Secretary and Treasurer of IEEE Antennas and Propagation Society Japan Chapter in 1998, the Secretary of Technical Committee on Electromagnetic Compatibility of IEICE from 2004 to 2006, the Secretary of Technical Committee on Antennas and Propagation of IEICE from 2008 to 2010. He has been an Associate Editor of *IEICE Transactions on Communications* since 2007.

Qiaowei Yuan received the B.E., M.E., and Ph.D. degrees from Xidian University, Xi'an, China, in 1986, 1989 and 1997, respectively.

From 1990 to 1991, she was a special research student at Tohoku University, Sendai, Japan. From 1992 to 1995, she worked in Sendai Research and Development Laboratories, Matsushita Communication Company, Ltd., engaging in research and design of the compact antennas for 2rd generation mobile phone. From 1997 to 2002, she was a Researcher in the Sendai Research and Development Center, Oi Electric Company, Ltd., engaged in the research and design of small antennas for pager communication and the parabolic antenna for 26.5 GHz fixed wireless access (FWA) communication. From 2002 to 2007, she was a Researcher with the Intelligent Cosmos Research Institute, Sendai, Japan, involved in the research and development of adaptive array antenna and RF circuits for mobile communications. From 2007 to 2008, she was an Associate Professor at Tokyo University of Agriculture and Technology. She is currently an Associate Professor at Sendai National College of Technology.

Dr. Yuan received the Best Paper Award and Zen-ichi Kiyasu Award in 2009 from the Institute of Electronics, Information and Communication Engineers (IEICE) of Japan.

Kunio Sawaya (SM'02) received the B.E., M.E. and Ph.D. degrees from Tohoku University, Sendai, Japan, in 1971, 1973 and 1976, respectively.

He is presently a Professor in the Department of Electrical and Communication Engineering at Tohoku University. His areas of interests are antennas in plasma, antennas for mobile communications, theory of scattering and diffraction, antennas for plasma heating, and array antennas.

Prof. Sawaya received the Young Scientists Award in 1981, the Paper Award in 1988, Communications Society Excellent Paper Award in 2006, and the Zen-ichi Kiyasu Award in 2009, all from the Institute of Electronics, Information and Communication Engineers (IEICE). He served as the Chairperson of the Technical Group of Antennas and Propagation of IEICE from 2001 to 2003, the Chairperson of the Organizing and Steering Committees of the 2004 International Symposium on Antennas and Propagation (ISAP'04), and the President of the Communications Society of IEICE from 2009 to 2010. He is a fellow of IEICE and a member of the Institute of Image Information and Television Engineers of Japan.

Tamami Maruyama (M'91) received the B.S. and M.S. degrees from Tsuda College, Tokyo, Japan, in 1985 and 1988, respectively, and the Ph.D. degree from Tohoku University, Sendai, Japan, in 2001.

She is a Senior Research Engineer at NTT DoCoMo Research Laboratories. In 1988, she joined Nippon Telegraph and Telephone (NTT) Corporation. In 2003, she joined NTT DoCoMo Inc. Her main research interests include optimum antenna design method, genetic algorithm, application of metamaterials and reflectarray for wireless communication, design of multi-frequency antennas for digital mobile communication base stations, small sector antennas for indoor high-speed wireless LANs and small multi-band antenna for handset applied genetic algorithm.

Dr. Maruyama received the Young Engineer Award from the IEEE AP-S Tokyo Chapter in 1995, an Excellent Paper Award from IEICE in 1998, and the Best Paper Award from ISAP 2007. She is a member of the Electronics, Information and Communication Engineers (IEICE) of Japan.

Tatsuo Furuno (M'95) received the B.S. degree from Niigata University, Japan, in 1986.

He joined Nippon Telegraph and Telephone (NTT) Corporation and engaged in the research and development of cordless telephone system, radio propagation characteristics for PHS (Personal Handy-phone System) and Wireless LAN. He joined NTT DoCoMo in 1999 and engaged in the research and development of public wireless LAN service, indoor radio propagation, and cognitive radio. He is currently a Senior Research Engineer at NTT DoCoMo Research Laboratories.

Shinji Uebayashi (M'82) received the B.E., M.E., and D.E. degrees in electronic engineering from Nagoya University, Nagoya, Japan, in 1981, 1983, and 1986, respectively.

From 1986 to 1992, he was with the NTT Laboratories, Yokosuka, Japan, where he worked on the development of digital cellular system (PDC). From 1992 to 2009, he was with NTT DoCoMo, Inc., where he worked on the development of the W-CDMA cellular system and EMC for cellular systems. He is presently a Professor in the School of Information Science and Technology, Chukyo University. His research interests include radio propagation, wireless communication and positioning.